J. Fluid Mech. (1978), *vol.* 86, *part* 1, *pp.* 109–127
Printed in Great Britain

Particle motions near the bottom in turbulent flow in an open channel

By B. MUTLU SUMER AND BEYHAN OĞUZ

Technical University of Istanbul, Faculty of Civil Engineering,
Taşkişla, Taksim, Istanbul, Turkey

(Received 11 September 1976 and in revised form 18 October 1977)

A photographic technique has been used to make observations of the motion of heavy suspended particles in an open channel with a smooth bottom. The observations showed that the path of an individual heavy particle consists of an alternation between upward and downward paths traced by the particle as it travels close to the bottom. The path records appear to reveal most of the flow patterns near the wall shown up by earlier visualization observations; the measured kinematical quantities concerning the particle motion are in accord with those of earlier observations (e.g. Nychas, Hershey & Brodkey 1973). Making use of the present observations and following Offen & Kline's (1975) model of the bursting process in turbulent boundary layers, an attempt was made to explain the mechanism of particle suspension close to the wall in turbulent flows.

1. Introduction

Recent turbulence observations have thrown light on the turbulence structure in the so-called wall region and outer region of turbulent boundary layers in some detail. Of these observations, the most recent ones are those by Nychas *et al.* (1973) and Offen & Kline (1973, 1974). In both Nychas *et al.* (1973) and Offen & Kline (1973) an extensive review was included. The observed repetitive nature of the flow patterns near the wall suggested a quasi-cyclic process: a deterministic sequence of events which occurs randomly in space and time.

As has been reported by many researchers, observations made in a laboratory channel show that a small heavy particle may be lifted from the bottom into the body of the flow and suspended. Such a particle, in suspension, travels most of the time close to the bottom (owing to gravity), but does not leave the main body of the flow. Hence there must be some mechanism which prevents the particle from settling on the bottom. One might expect that this mechanism is closely associated with the sequence of events in the wall region mentioned in the preceding paragraph.

To the writers' knowledge, Sutherland (1967) was the first investigator who tried to explain particle entrainment by turbulent flows by making use of turbulence observations near the wall (entrainment in Sutherland's study was considered to include both the initiation of particle motion and the suspension of particles by the flow). By writing the equation of motion for a grain and taking an ensemble average, Engelund (1970) obtained an expression which consists of gravity, drag and pressure-gradient terms, the pressure being the mean deviation from the static pressure. Using the measured distribution of the intensity of turbulence in the vertical direction close

to the wall, Engelund interpreted this expression as follows. If the pressure-gradient term exceeds the reduced gravity, the conditions close to the wall will be as in a reversed gravity field, i.e. the central part of the wall region constitutes a 'barrier' against settling. Grass (1974) recorded the details of the suspension process in a turbulent boundary layer on a flat plate. His work showed that sand particles were carried up from the bed region through virtually the total boundary-layer thickness. To explain the mechanism which is responsible for the suspension of particles, especially relatively heavy ones, Batchelor (1965) suggested that more observations of the motion of heavy suspended particles under controlled conditions are needed. He suggested, in particular, that it would be especially valuable to make observations of the motion of a single heavy particle, the 'concentration' then being interpreted as the probability density in a cross-sectional plane of particle position, because that would avoid the possible complication of the suspended solid material exerting an influence on the turbulence, especially near the bed. This idea stimulated the research presented in this study, in which a photographic system was used to observe the motion of heavy suspended particles in an open channel with a smooth bottom.

The photographic system is described in § 2. With the aid of the recorded data, a description of the observed particle paths is given in § 3. As has previously been stated, there must be a close connexion between the mechanism of particle suspension and the sequence of events in the wall region. From recent observations (particularly those of Nychas *et al.* 1973; Offen & Kline 1973), the model given by Offen & Kline (1975) associated with the deterministic sequence of events in the wall region, and the present observations of heavy suspended particles described in § 3, a mechanism of the particle suspension is proposed in § 4.

2. The experimental facility

2.1. *The flow*

The $56 \times 30 \times 650$ cm flume used in the experiments, located in the I.T.U. Hydraulics Laboratory, has an adjustable slope. Its bottom and side walls are made of glass; the former was painted black for photography. There exists a sharp-crested weir at the upstream end of the flume to measure the flow rate and a vertical sluice gate at its downstream end to adjust the flow depth. The depth of flow was kept constant at 9·2 cm for the tests. The mean flow velocity was calculated from the volumetric discharge divided by the cross-sectional area and kept constant throughout the tests at approximately 23·2 cm/s. The flow Reynolds number, based on the mean flow velocity and flow depth, was approximately 19000. The shear velocity was predicted as 1·2 cm/s from the Darcy–Weisbach equation $u_* = U_m(\frac{1}{8}f)^{\frac{1}{2}}$, where $f = 0{\cdot}316/Re^{\frac{1}{4}}$ since $Re < 10^5$ (Henderson 1966, p. 93). Here Re is the Reynolds number based on the mean flow velocity and hydraulic radius: $Re = 4RU_m/\nu$.

To flatten the lateral mean velocity profile, a vertical row of rods was fixed close to the inlet section. The two-dimensionality of the flow was checked by employing a miniflowmeter which was traversed across the flume at fourteen heights (from 0·75 cm to 7 cm) above the bottom. These measurements showed that the local mean streamwise velocity varied by less than 4% over the centre 20 cm of the flume width.

To make the flow fully developed as close to the entrance of the flume as possible, roughness elements were fixed on the bottom at the inlet of the flume. Mean velocity

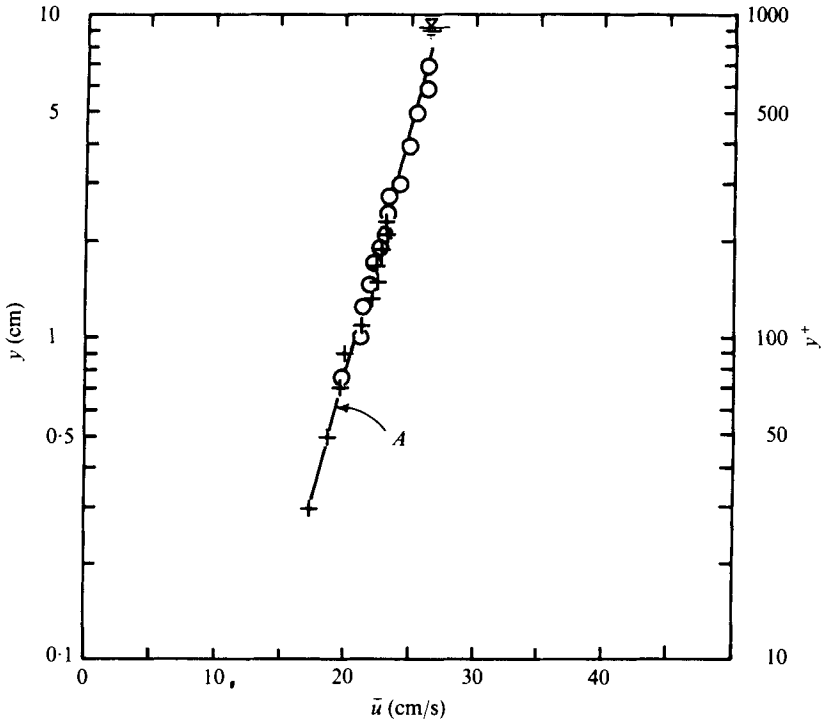

FIGURE 1. Mean velocity profile at the centre at the station 3 m downstream from the flume entrance. ○, velocities measured by miniflowmeter; +, velocities measured by the fixed camera system employed in the main tests; *A*, logarithmic velocity profile $\bar{u} = u_*(2{\cdot}4 \ln y^+ + 5{\cdot}8)$.

profiles were measured along the centre-line of the flume at four stations (1 m apart) and compared with the logarithmic velocity profile (Monin & Yaglom 1971, pp. 276–277) $\bar{u}(y^+) = u_*(2{\cdot}4 \ln y^+ + 5{\cdot}8)$, y^+ being in the interval $30 < y^+ < 1000$. The measured profiles agreed quite well (figure 1) with the logarithmic distribution at all stations except the one 1 m downstream from the entrance; even at this station, the agreement was good up to a height of 5 cm above the bottom.

2.2. *The particles*

In choosing the particles, the most important factor was the need that the particles should stay in suspension. This implies that (*a*) the parameter $w/\kappa u_*$ is not much greater than unity (herein w is the terminal fall velocity of the particle in quiescent fluid, u_* is the shear velocity and κ is the Kármán constant) and (*b*) the particle is big enough to be exposed to the action of the turbulence outside the viscous sublayer (Sumer 1974). The latter is a condition which could readily be met. As far as condition (*a*) is concerned, once the flow has been chosen, only the settling velocity of the particle need be determined in order to satisfy condition (*a*). Although the plastic spheres available in industry have densities slightly greater than that of water, this condition cannot be met. To obtain particles with extremely small settling velocities, it was necessary to produce them ourselves. In a fashion similar to the work of Batchelor, Binnie & Phillips (1955), the particles were made of adhesive wax. The material was weighed out to give a sphere of the required size and shaped into spherical form by

Particle	Particle diameter d (mm)	d^+	Measured settling velocity in quiescent water w (cm/s)	Water temperature (°C)	Settling velocity parameter $w/\kappa u_*$	Camera system used	Velocity data obtained
A	3·1	34	0·22	16·0	0·44†	Camera system moving along the flume	Instantaneous vertical velocities of particles
B	4·0	44	0·85	16·4	1·67†		
C	2·8	28	0·77	13·5	1·52†	Fixed camera system	Instantaneous longitudinal and vertical velocities of particles

† κ (the Kármán constant) is taken to be 0·42.

TABLE 1. Particle parameters.

rubbing between the fingers. The spheres were then painted white, still being lighter than water. Grains of fine sand were then pressed into the particles until the measured settling velocity was such that condition (*a*) was met. The particle properties are given in table 1.

2.3. *Apparatus and instrumentation*

Two types of camera system were used in the experiments: (*a*) a camera system which moved along the flume at a constant speed and (*b*) a camera system which was fixed at a particular station.

The moving camera system, which had been used to record the plan-view motion of particles in an earlier study (Sumer 1977), was designed to move along the flume at a constant speed of 23·3 cm/s so as to trace and record the vertical motion of the particle through the glass side wall of the channel; this was achieved by deflecting the light paths through three mirrors at 45° to the horizontal. The system consisted of two units: a conventional 35 mm camera and a stroboscope. A conventional 35 mm camera was manipulated so as to maintain a continuously open shutter. A motorized drive, attached to the wind-on spool of the camera, propelled the film past the open shutter at a speed of 1·8 cm/s. To reduce the over-exposure of the film, the particle was painted white and the background side wall black. The camera was fixed to the trolley such that it viewed the plan of the flume. The stroboscope consisted of a flash tube, Strobex Lamp Model 70, coupled with a Strobex Power Supply Model 99 from Chadwick–Helmuth Co. Inc. The flash-tube unit was fixed to the trolley such that the light coming from it illuminated the area where the particle was to be photographed, the light path making an angle of about 30° with the side wall of the channel. Thus the light reflected from the glass side wall was not allowed to pass through the camera lens (figure 2).

The moving camera system was not capable of giving the particle path accurately in the streamwise direction. In order to obtain instantaneous longitudinal and vertical velocities of particles simultaneously, a second type of camera system was employed; this consisted of (*a*) a stroboscope and (*b*) a 35 mm camera located 3 m downstream from the flume entrance and fixed so as to view the particle paths through the glass side wall of the flume.

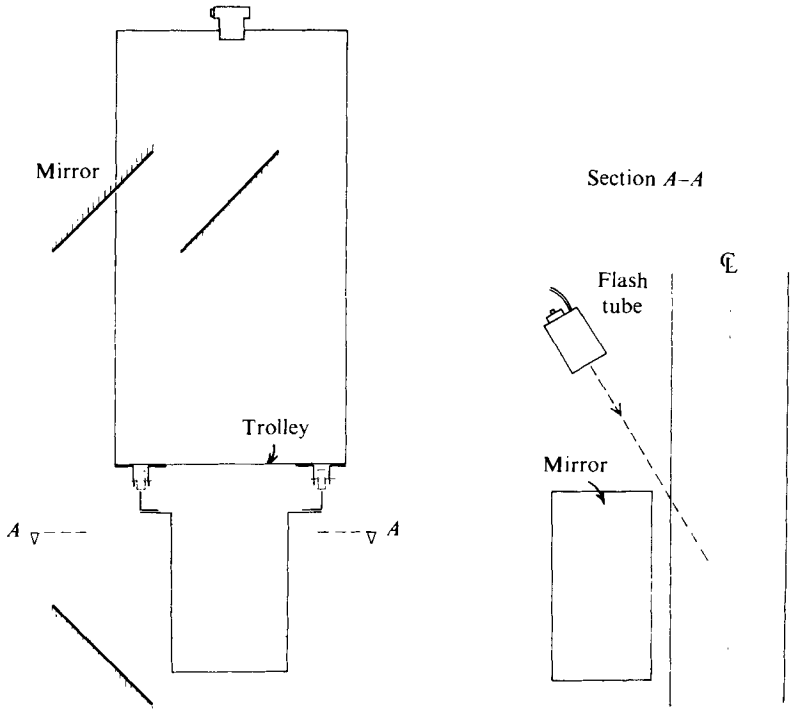

FIGURE 2. Schematic diagram of the cross-section of the experimental flume and the camera system moving along the flume.

When a particle was photographed using the moving camera system, the following experimental procedure was adopted. The trolley was moved to the entrance of the flume. The stroboscope was activated in the dark. A rubber hose of diameter 7 mm (31 cm in length) containing water and the particle, the particle being in the body of the water, was immersed in the flow and held at some point in the vicinity of the upstream end of the area illuminated by the flash. The water and the particle in the hose were instantaneously flushed into the main body of the flow in the opposite direction to the stream. At the same instant the trolley was made to move along the flume and the film was made to travel. As the flash glowed, the particle image detected on the film was immediately recorded. After the flash went out, nothing was recorded. This made it possible to record the side-view motion of the particle as a series of dots on film strips (see figure 3). After the particle had been released into the body of the flow and photographed, it was retrieved at the downstream end of the flume. One such particle was used repeatedly. A similar procedure was adopted using the fixed camera system. Two typical records obtained via the latter technique are shown in figure 4 (plate 1).

Recording in the experiments was done at flash frequencies of 12–16 Hz. The x and y co-ordinates of the particle images on film strips were measured using an aviograph (Aviograph Wild B8S) interfaced to a recorder (Wild EK8) which was coupled with an IBM typewriter. Film readings were made for several film strips and lists of printed co-ordinates obtained with the aid of this technique were then analysed.

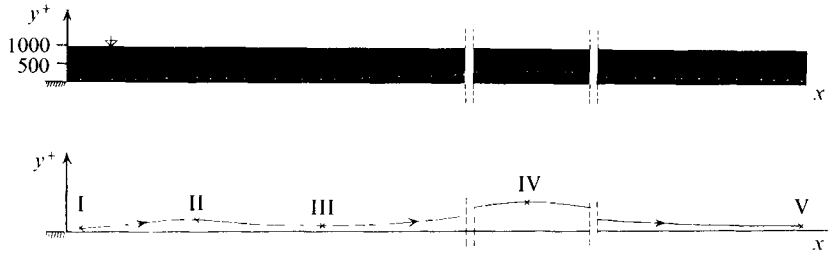

FIGURE 3. Typical particle path recorded by the moving camera system. Particle A. Exposures are spaced 0·087 s apart. I, $y^+ = 36$; II, $y^+ = 107$; III, $y^+ = 71$; IV, $y^+ = 338$; V, $y^+ = 80$. Note that the particle images are accurately recorded in the y direction but not in the x direction.

Particle	y_{0r}^+	y_t^+
A	87*	209
	60*	224
	54*	214
	17 (from the bottom)	134
	27	152
	17 (from the bottom)	194
	36*	107
	71	338
B	61*	219
	44	131
	61*	148
	22 (from the bottom)	114
	43*	252
C	49	120
	61*	112
	18*	105
	64*	129
	14 (from the bottom)	59
	26	96
	37*	123
	28*	112
	18*	94
	32	155
	59*	100

TABLE 2. y^+ at termination of the upward paths of individual particles, y^+ at the origin of the upward paths being in the zone of the wall region where the wall-area ejections originate. $y_{0r}^+ = y^+$ at origin; $y_t^+ = y^+$ at termination; y_{0r}^+ with asterisk $= y^+$ where particle entered the viewing area of the camera at this position.

3. Observations of particle motion

3.1. *A brief description of the vertical motion of a single particle close to the bottom*

In this subsection, with the aid of the recorded data, a brief description of the observed particle paths in the vertical direction is given. Throughout the description, the particle position in the vertical is expressed in terms of the non-dimensionalized distance y^+ from the bottom, where $y^+ = yu_*/\nu$.

Particle	Run	y_{0r}^+	y_t^+	$\bar{y}^+$	U (cm/s)	$\bar{u}(\bar{y}^+)$ (cm/s)	V (cm/s)
A	36/025/1	17 (from the bottom)	134	76	—	—	1·13
	37/24/1	17 (from the bottom)	194	106	—	—	1·18
	36/025/3	27	152	90	—	—	0·89
	36/223/1	54*	214	134	—	—	1·91
	35/930	60*	224	142	—	—	1·17
	37/151/3	71	338	205	—	—	1·10
B	30/21/1	22 (from the bottom)	114	68	—	—	0·73
	30/26/3	22 (from the bottom)	79*	50	—	—	1·53
	30/13/1	43*	252	148	—	—	1·49
	28/2829/1	44	131	88	—	—	1·01
	30/26/1	61*	148	105	—	—	0·94
C	122	61*	112	87	18·63	19·99	0·50
	125	32	155	94	18·95	20·21	2·18
	129	18*	105	62	18·17	19·00	1·30
	204	64*	129	97	19·38	20·30	1·51
	206	14 (from the bottom)	59	37	12·47	17·50	1·55
	215	26	96	61	16·13	20·27	1·36
	327	28*	112	70	16·94	19·36	1·07
	332	18*	94	56	16·02	18·71	1·27

TABLE 3. Some data on wall-area paths of individual particles rising through the water body. y_{0r}^+ and y_t^+ are y^+ at the origin and at termination of the rising path, respectively; $\bar{y}^+ = \frac{1}{2}(y_{0r}^+ + y_t^+)$; U = average value of the longitudinal velocity of an individual particle over its path; $\bar{u}(\bar{y}^+)$ = mean velocity calculated from the logarithmic velocity distribution; V = average value of the vertical velocity of an individual particle over its path. For a y_{0r}^+ with an asterisk, the particle entered the viewing area of the camera at this position; for a y_t^+ with an asterisk, the particle left the viewing area of the camera at this position.

We shall begin the description with a particle which starts to travel upwards from the region $0 < y^+ < 50$ (the zone $0 < y^+ < 50$ is part of the wall region where the so-called wall ejections originate, Nychas *et al.* 1973). Such a particle, in a single continuous motion, reached a y^+ between 100 and 200 (table 2). The particle then began a downward excursion (towards the bottom) as its upward motion terminated. The downward motion continued down to a relatively smaller y^+, sometimes at the bottom, where the particle started another upward motion. For example, one particle was lifted up from the bottom and carried through a distance of 134 in y^+ units. It then returned towards the wall region, its downward path terminating at $y^+ = 27$. From this position the particle started another upward motion. As another example, one particle which entered the viewing area of the camera at $y^+ = 36$ reached a y^+ of 107 then started to travel downwards to a y^+ of 71. From this position it started to rise again and its upward path terminated at $y^+ = 338$. In tables 3 and 4, some data on wall-area particle paths are presented.

3.2. *Some relevant measurements*

The data obtained from film records were used to predict the probability density function of the projection on a cross-sectional plane of the particle position. Histograms representing the probability density distributions are shown in figure 5. In the case of particle *A*, the following expression, obtained from the balance between the

Particle	Run	y_{0r}^+	y_t^+	$\bar{y}^+$	U (cm/s)	$\bar{u}(\bar{y}^+)$ (cm/s)	V (cm/s)
A	37/151/2	107	71	89	—	—	−0·95
	36/025/2	134	27	80	—	—	−0·96
	35/6276/6	209	70	140	—	—	−1·00
	35/6276/2	314	87	200	—	—	−0·93
B	30/21/2	114	35*	75	—	—	−2·96
	28/2829/2	131	22 (at the bottom)	77	—	—	−4·26
	30/26/2	148	22 (at the bottom)	85	—	—	−1·16
	28/293/2	219	157*	188	—	—	−1·85
	30/13/2	252	52*	152	—	—	−1·04
C	107	108	36	72	20·75	19·44	−1·03
	111	160	81	121	24·09	20·94	−1·30
	204	129	48*	89	24·93	20·05	−1·57
	211	39	14 (at the bottom)	27	21·44	16·59	−0·70
	212	99*	23	61	21·81	18·96	−1·25
	223	63*	22	43	19·07	17·94	−1·19
	329	128	14 (at the bottom)	71	19·40	19·39	−1·47

TABLE 4. Some data on wall-area paths of individual particles falling through the water body. Symbols in table 3.

transport due to a settling velocity and the turbulent transport in the equilibrium case, is considered for comparison (Elder 1959):

$$p(\eta) = \frac{\sin \pi\beta}{\pi\beta}\left(\frac{1-\eta}{\eta}\right)^{\beta}, \quad \beta < 1, \tag{1}$$

in which $\eta = y/h$, $\beta = w/\kappa u_*$ and h is the flow depth. The agreement appears to be reasonable. The histograms indicate that particle A can reach a y^+ of about 500–550, whereas particles B and C can hardly be expected even to reach a y^+ of about 300 owing to the gravity effect.

Some data on individual particle paths are presented in tables 3 and 4. In the tables, U is an average velocity in the sense that it was predicted as the average value, over the particle path, of the longitudinal velocity of the particle. Similarly, V is the average value, over the particle path, of the vertical velocity of the particle. Nychas *et al.* (1973, tables 1–4) presented some data on the wall-area ejections and transverse vortices. Comparison of the non-dimensionalized velocities v/u_* of Nychas *et al.* with those of the present work shows that they are of the same order (since these velocities belong to individual particles, comparison in a strict sense is not possible).

Data on the particle ejection velocity from the present study are plotted in figure 6 together with the data on a suspension of fine sand obtained by Grass (1974) and also the ejection-velocity data presented by Brodkey, Wallace & Eckelmann (1974, figure 11). In this figure, the data corresponding to particles A and B of the present study are the single-particle ejection velocities V plotted against $\bar{y}^+$ (for notation, see table 3). In the case of particle C, for the sake of clarity the ejection-velocity data were plotted in the following manner as there were some forty-five (V, $\bar{y}^+$) pairs in the narrow interval $20 < y^+ < 120$. This interval was divided into small increments of $\Delta y^+ = 20$. At each increment, the average $\langle V \rangle$ and the standard deviation σ_V of the sample of V velocities were predicted and plotted in figure 6. Grass' data in the same figure

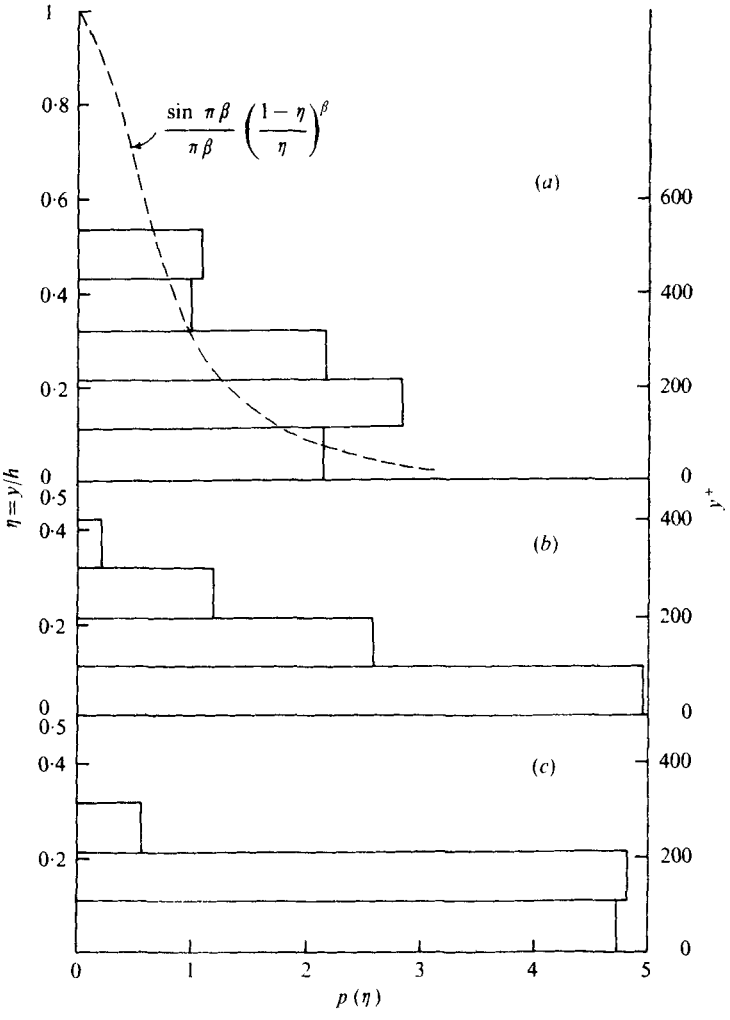

FIGURE 5. Histograms representing the probability density distribution of particle position in the vertical. (*a*) $w/\kappa u_* = 0{\cdot}44$ (particle A; total sample size = 400); (*b*) $w/\kappa u_* = 1{\cdot}52$ (particle C; total sample size = 1239); (*c*) $w/\kappa u_* = 1{\cdot}67$ (particle B; total sample size = 311).

represent the average ejection velocities based on measurements of individual continuous ejections of fine sand particles (in Grass' measurements, the parameter $\beta = w/\kappa u_*$ was 1·1 and the ratio δ/d of the thickness of the viscous sublayer to the particle size was 1·2, where $\delta = 5\nu/u_*$). Note that in Grass' observations ejection events in the bursting process were visualized by the sand; thus Grass' work appeared to establish a direct link between the fluid ejection process and the particle suspension. Finally, the Brodkey *et al.* data in figure 6 constitute a plot of the mean of the velocity component normal to the wall (corresponding to an ejection type of motion) *vs.* wall distance. Brodkey *et al.* considered the ejection type of motion to be associated with the following category of the truncated u and v signals: $u < \overline{u}$ and $v > 0$, in which u is the instantaneous velocity in the longitudinal direction, $\overline{u}$ is the mean local velocity and v is the instantaneous velocity in the direction perpendicular to the wall. Of the

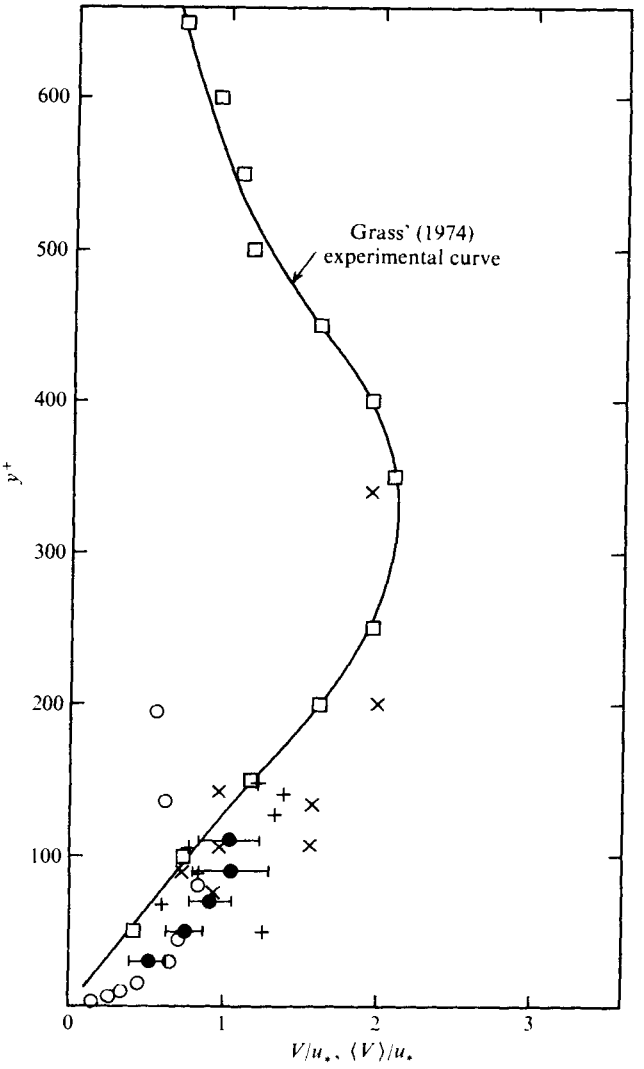

FIGURE 6. Ejection-velocity data plotted against y^+. ×, +, particles A and B, respectively, average value V of ejection velocity of individual particle over the particle path; ●, particle C, average of the sample of V velocities at a particular depth increment, the error bar denoting the standard deviation of the sample; □, Grass (1974), average ejection velocities of fine sand particles; ○, Brodkey *et al.* (1974, figure 11), mean of the fluctuating velocity component normal to the wall corresponding to ejection type of motion.

data of Brodkey *et al.* plotted in figure 6, those corresponding to $y^+ = 135$ and $y^+ = 195$ differ from the general trend observed in this figure. The writers believe that the discrepancy is due to the fact that the positions $y^+ = 135$ and $y^+ = 195$ were both located in the central part of the oil channel used by Brodkey *et al.* (in fact, $y^+ = 195$ corresponds to the centre of the channel, i.e. $y/b = 1$, where b is the half-width of the channel); then any motion detected at these positions would have been influenced by the bursting process in the other half of the channel.

As is seen from figure 6, the data on the particle ejection velocity from the present work seem to be in good agreement with the information at present available.

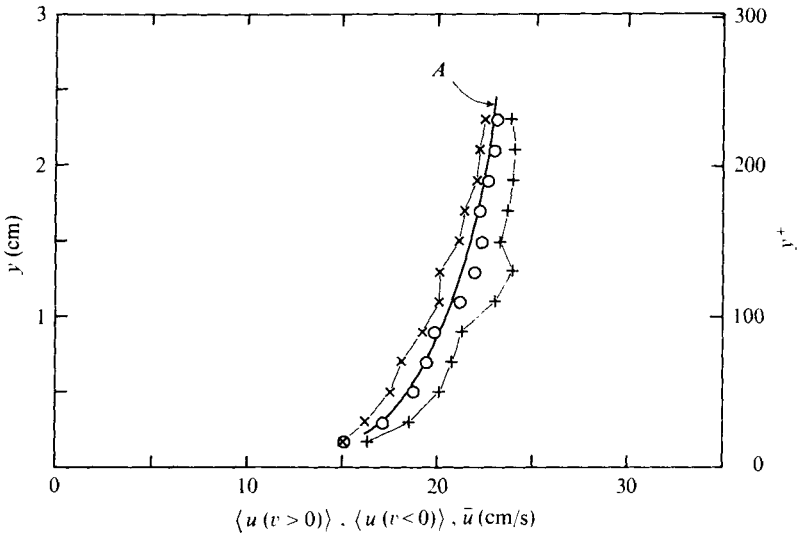

FIGURE 7. Conditionally averaged streamwise velocity profiles. Particle *C*. ×, $\langle u(v > 0)\rangle$, average of the conditional sample of u velocities corresponding to $v > 0$ (ejection correlation); +, $\langle u(v < 0)\rangle$, that corresponding to $v < 0$ (sweep correlation); ○, the overall average of u velocities (the mean velocity); *A*, the logarithmic velocity profile $\bar{u} = u_*(2{\cdot}4 \ln y^+ + 5{\cdot}8)$.

3.3. *Conditionally averaged streamwise velocity profiles*

The co-ordinate data obtained through the technique described in § 2.3 were processed to yield sequential pairs (u,v) of instantaneous longitudinal and vertical particle velocities. The flow depth was divided into small increments of $\Delta y = 0{\cdot}2$ cm. For each instantaneous (u,v) pair, the depth increment in which this particular (u,v) pair occurred was determined. Each (u,v) pair was stored in the computer in the form of an array for the depth increments given in table 5. At each increment, the conditional sampling procedure adopted in the present study selected u velocities of the following three types: (*a*) those corresponding to $v > 0$, (*b*) those corresponding to $v < 0$ and (*c*) those corresponding to $v = 0$. Note that the statistical properties (of the conditional samples) predicted at the upper depth increments are expected not to be as reliable as those at the lower depth increments, since the sample sizes at the upper depth increments appear to be far smaller than those at the lower depth increments. (This is because the particle (particle *C*) tends to travel most of the time within the lower depth increments; see figure 5*b*.)

Ensemble averages of the conditional samples of instantaneous u velocities corresponding to $v > 0$, $v < 0$ and $v = 0$ occurring at the various depth increments are denoted by $\langle u(v > 0)\rangle$, $\langle u(v < 0)\rangle$ and $\langle u(v = 0)\rangle$, respectively (table 5). Note that $u(v > 0)$ is the streamwise velocity of the particle as it rises and $u(v < 0)$ is that as it falls through the water. $u(v = 0)$ is the streamwise velocity of the particle as it travels almost horizontally along the crests or troughs of its path. The overall average of u velocities for each increment is denoted by $\bar{u}$. The conditionally averaged velocities $\langle u(v > 0)\rangle$ and $\langle u(v < 0)\rangle$ and the overall average $\bar{u}$ are plotted in figure 7, in which the logarithmic velocity profile (Monin & Yaglom 1971, pp. 276–277) $\bar{u} = u_*(2{\cdot}4 \ln y^+ + 5{\cdot}8)$ is also plotted for comparison.

Depth increment		$\langle u(v>0)\rangle$	$\sigma_{u(v>0)}$	$\langle u(v<0)\rangle$	$\sigma_{u(v<0)}$	$\langle u(v=0)\rangle$	$\sigma_{u(v=0)}$	$\bar{u}$	Total sample sizes			
Δy (cm)	Δy^+	(cm/s)	(cm/s)	(cm/s)	(cm/s)	(cm/s)	(cm/s)	(cm/s)	$N_{u(v>0)}$	$N_{u(v<0)}$	$N_{u(v=0)}$	N
0·14†–0·2	14–20	15·09	2·13	16·29	3·24	14·00	2·54	15·10	20	13	14	47
0·2–0·4	20–40	16·16	2·53	18·53	3·15	17·01	3·16	17·10	99	70	67	236
0·4–0·6	40–60	17·45	2·73	20·10	3·19	18·49	3·30	18·66	71	63	29	163
0·6–0·8	60–81	18·11	2·67	20·68	3·09	19·71	2·05	19·36	52	44	18	114
0·8–1·0	81–101	18·99	2·22	21·24	2·94	19·19	1·92	19·81	60	40	13	113
1·0–1·2	101–121	20·13	2·19	23·03	3·44	20·64	1·81	21·18	46	32	20	98
1·2–1·4	121–141	20·07	2·59	23·91	2·11	22·23	2·71	21·89	27	23	9	59
1·4–1·6	141–161	21·21	2·60	23·21	2·20	22·87	2·24	22·32	31	31	13	75
1·6–1·8	161–181	21·40	2·46	23·57	2·31	21·44	1·87	22·08	31	20	13	64
1·8–2·0	181–202	22·04	2·19	23·89	2·14	21·15	3·63	22·60	35	21	5	61
2·0–2·2	202–222	22·23	1·95	23·96	1·87	23·14	2·23	22·92	30	18	8	56
2·2–2·4	222–242	22·52	1·52	23·79	2·38	22·39	2·34	22·98	25	21	9	55

† $y = 0{\cdot}14$ cm is the distance of the centroid of the particle from the bottom when the particle sits on the bottom.

TABLE 5. Data on conditionally averaged streamwise velocities. Particle *C*. $\langle u(v>0)\rangle$, $\sigma_{u(v>0)}$, average and standard deviation of the conditional sample of u velocities corresponding to $v>0$, respectively; $\langle u(v<0)\rangle$, $\sigma_{u(v<0)}$, average and standard deviation of the conditional sample of u velocities corresponding to $v<0$, respectively; $\langle u(v=0)\rangle$, $\sigma_{u(v=0)}$, average and standard deviation of the conditional sample of u velocities corresponding to $v=0$, respectively; $\bar{u}$, overall average of u velocities at a particular depth increment; $N_{u(v>0)}$, $N_{u(v<0)}$, $N_{u(v=0)}$, total sizes of the conditional samples of u velocities corresponding to $v>0$, $v<0$ and $v=0$, respectively; N, total size of the sample of u velocities at a particular depth increment.

The conditionally averaged streamwise velocity profiles of the present study are remarkably similar in shape and relative magnitude to those presented by Nychas *et al.* (1973, figure 6). It should be noted that Nychas *et al.* obtained their profiles from their observations of actual ejection and sweep events where the latter events could be made visible with the aid of very small suspended solid particles.

4. A proposed mechanism of the particle suspension close to the bottom

4.1. *Offen & Kline's model of the bursting process in turbulent boundary layers*

Experiments by Corino & Brodkey (1969), Grass (1971), Nychas *et al.* (1973) and others have shown that the wall region in turbulent flow consists of two zones each of which has its own structural character.

(*a*) *Viscous sublayer.* The flow in this region has a streaky character; very large lateral variation in the streamwise component of the velocity is correlated with the lateral velocity. This zone is reported to be the region $0 \leqslant y^+ \leqslant 5$, of which the lowermost part $y^+ < 2{\cdot}5$ is essentially passive and the rest active.

(*b*) *Generation region.* This region coincides with the position of the majority of the so-called fluid ejection and sweep phases. Major generation and dissipation of turbulence occur in this region. According to Corino & Brodkey, the generation region is the zone $5 \leqslant y^+ \leqslant 70$.

The above-mentioned experiments have also shown that the nature of the flow pattern near the wall is repetitive; a deterministic sequence of events occurs near the wall (although these events occur randomly in space and time). Ejections and sweeps are two phases of this sequence. In the ejection phase low-speed fluid is ejected away from the wall in the form of a three-dimensional disturbance. Ejected fluid originates from the lower zone of the generation region and has an instantaneous velocity component perpendicular to the wall which is as high as 30% of the longitudinal component. In the sweep phase high-speed fluid penetrates towards the wall, again in the form of a three-dimensional disturbance.

Taking into consideration that (*a*) the repetitive nature of the flow patterns near the wall suggested a quasi-cyclic process and (*b*) enough information on the behaviour of the basic flow structures had been collected to attempt a synthesis, Offen & Kline (1973, 1975) have proposed a model explaining the complete cycle of events. Their model will be described herein very briefly (with the help of figure 8, which is a slightly different version of Offen & Kline's figure 1, 1975; figure 5.1, 1973), because of its direct applicability.

The region where the low-speed fluid ejection originates appears to be of the form of a streak near the wall. Offen & Kline viewed this low-speed wall streak as a sub-boundary layer within the conventionally defined turbulent boundary layer. Also they viewed the lift-up of the wall streak (i.e. the ejection of low-speed fluid) as an upwelling motion of this sub-boundary layer which is similar to a local separation due to a temporary local adverse pressure gradient. Immediately after the wall streak is lifted up, a local convected recirculation cell will form below the lifted streak (figure 8*a*). As the ejection progresses, both the lifted fluid and the recirculation cell will move away from the wall and grow in size (figure 8*b*). The flow along the lowest portion of the convected cell will be in the reverse direction with respect to an observer moving

with the convection speed of this recirculation cell. The relative reverse flow near the wall implies that the fluctuating pressure field there is temporarily characterized by a local adverse pressure gradient. When this structure passes over a low-speed wall streak, the correct conditions will exist for another lift-up; i.e. the next lift-up will occur as this structure continues to pass overhead (figure 8*d*). The previously lifted fluid breaks up as it interacts with the next lifting wall streak (figure 8*e*). The whole sequence of events during the lifetime of a wall streak (i.e. (*a*) the appearance of the wall streak, (*b*) the growth of this wall streak, leading to its lift-up from the wall, and (*c*) the breakup of any signs of coherency in the visual representation of this structure) is called 'bursting'. The flow structure which consists of the lifted fluid and its associated recirculation cell is called a burst. As has already been mentioned, the breakup of a burst occurs as it interacts with the next burst. Some fluid from both bursts returns to the wall, where it spreads out sideways, is quickly retarded and may be the source of new low-speed streaks further downstream. It should be noted that the previous burst would be made visible as a sweep by visualization devices located away from the wall (in the logarithmic region) near the origin of the new burst (see Offen & Kline 1975, figure 1*c*). Sweeps are therefore thought to represent the passage of the previous burst from further upstream. Offen & Kline's model summarized in this paragraph appears to be consistent with the trends in all the relevant data.

4.2. *Lift-up of the particle into the body of the flow: mechanism of the particle suspension close to the bottom*

We shall begin the description of the proposed mechanism with a particle which is on the bottom. The flow pattern very close to the bottom consists of a spanwise alternation of low-speed streaks and high-speed zones of fluid. When the high-speed fluid hits the bottom, it spreads out sideways. Spreading fluid pushes the particle (wandering in its immediate vicinity) to the adjacent low-speed wall streak; i.e. the particle finds itself swept into a low-speed wall streak. Several pieces of evidence support this argument. The first line in table 5 gives some data on the streamwise velocity of particles just leaving or just landing on the bottom. As is seen, the average streamwise velocity of particles leaving the bottom, $\langle u(v > 0)\rangle$, appears to be lower than that of particles landing on the bottom, $\langle u(v < 0)\rangle$. This implies that a particle leaving the bottom is in a low-speed zone; in fact, in the present experiments, streamwise velocities of individual particles as low as 9·8 cm/s were observed when particles were just leaving the boundary, as opposed to the fact that particles had streamwise velocities as high as 22·6 cm/s when landing there. A second piece of evidence comes from Engelund & Gravesen's (1972) work; they took photographs through the glass bottom of a channel in which very fine sediment was transported in suspension, sediment particles being sporadically in contact with the bottom plate. In their figure 2, areas covered by sediment particles, which were apparent on the bottom plate earlier than other particles, form a series of parallel streaks in the streamwise direction; the streaks are spaced in approximate agreement with $\lambda = 100\nu/u_*$, which is the reported value of the distance between low-speed wall streaks. A third piece of evidence concerns Jackson's (1976) argument. Referring to Williams & Kemp (1971, p. 515), Grass (1971, p. 250) and others, Jackson (1976, p. 551) spoke of alternating 'lanes' (parallel to the mean flow) of faster-moving, clear fluid and of slow, sediment-

laden fluid, the lanes being spaced in accordance with $\lambda = 100\nu/u_*$. Continuing his argument, Jackson (1976, p. 551) pointed out that 'the fact that high-speed streaks preferentially suffer sweeps whereas low-speed streaks undergo lift-up also favours this scheme, in the following manner: to preserve continuity, fluid nearest the bed must be transported laterally from high-speed streaks to low-speed streaks, which would account for grain segregation into the latter'.

On the other hand, if the particle size is such that it projects above the edge of the viscous sublayer (particularly above the edge of the passive zone of the viscous sublayer, $\delta_{\text{passive}} = 2{\cdot}5\nu/u_*$), it will be exposed to the action of the mechanism which brings about the lift-up of the low-speed wall streak. Indeed, if the particle size is less than the thickness of the viscous sublayer, it is hardly expected to be lifted into the body of the flow. The experimental evidence reported by Corino & Brodkey (1969, p. 18) reveals this fact: 'there was often a connected movement of (fluid) particles (in the passive zone of the viscous sublayer) which occurred simultaneously with the ejection (the lift-up of the wall streak), but rarely did they possess sufficient velocity to escape from the region'.

The fact that (*a*) a particle on the bottom finds itself swept into a low-speed wall streak and (*b*) it is projected above the edge of the viscous sublayer makes it possible for the particle to be subject to the action of the mechanism which brings about the lift-up of the wall streak. Following Offen & Kline's (1975) model, this mechanism is the temporary local adverse pressure gradient imposed on the wall streak by the burst passing overhead. The particle will then be subjected to and will respond to the pressure gradient producing fluid ejection zones. The conditionally averaged streamwise velocity profiles of the present experiments (table 5 and figure 7) support this hypothesis, since the 'rise' profile† in figure 7 shows a defect relative to the mean velocity profile (ejection correlation). Note that the previously mentioned similarity (see § 3.3) between the present velocity profiles in figure 7 and the Nychas *et al.* (1973, figure 6) data (obtained from the actual observed bursting events) additionally strengthens the latter argument. Grass (1976, private communication) pointed out, referring to his tests (Grass 1974), that the streamwise velocity profile measured using the ejected fine-sand flow tracer indicated a similar trend. The photographs of particle paths (figure 4) implicitly support the above hypothesis; as is clearly seen, the streamwise velocity of a particle rising through the water body appears to be less than that as the particle falls, since the time intervals between the particle images are kept constant throughout the particle path. Another piece of evidence supporting the above hypothesis comes from figure 6; the agreement between the data on the particle ejection velocity of the present study, the data on a suspension of fine sediment of Grass (1974) and the ejection-velocity data of Brodkey *et al.* (1974) supports the hypothesis that the particle is subjected to and responds to the same mechanism as produces fluid ejection zones.

† Comparison of $\langle u(v > 0)\rangle + \frac{1}{2}\sigma_{u(v>0)}$ values with the overall average $\bar{u}$ values at each depth increment (see table 5) suggests that the 'rise' profile presented in figure 7 includes not only the pure ejection type of motion ($v > 0$ and $u < \bar{u}$) but also what Brodkey *et al.* (1974) called the interaction (outward) type of motion ($v > 0$ and $u > \bar{u}$). Hence, if one adopts a further conditional sampling procedure which selects u velocities corresponding to $v > 0$ and $u < \bar{u}$, the 'rise' profile of this new conditional sampling procedure will show an even more pronounced defect relative to the mean velocity profile. Note that similar considerations apply to the 'fall' profile too; the result would be that the 'fall' profile shows a more pronounced excess relative to the mean velocity profile.

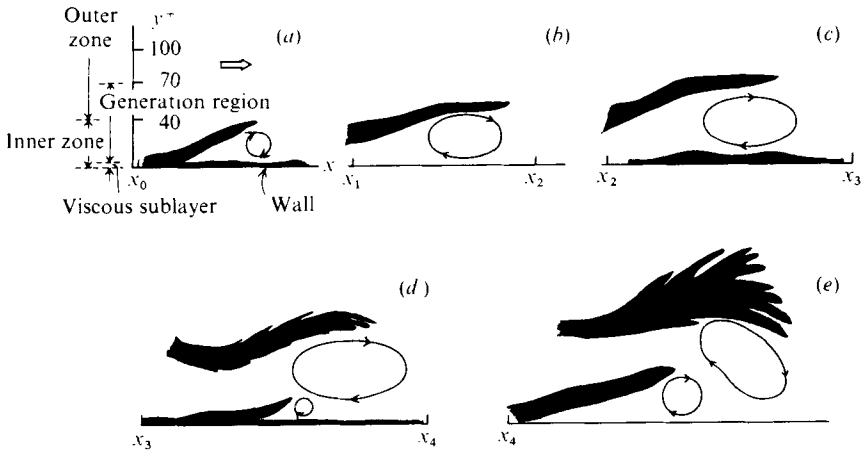

FIGURE 8. Instantaneous views of a burst (adopted from Offen & Kline 1973; figure 5.1; 1975, figure 1).

As has been described in § 3.1, the present observations showed that ejected heavy particles whose paths originated in the region $0 < y^+ < 50$ could reach a y^+ of 100–200. Since Nychas *et al.* (1973) reported that 'in some cases it was observed that ejected (fluid) particles (originating in the region $0 < y^+ < 50$) reached a y^+ of 200... Most of the ejected (fluid) particles observed reached a y^+ of 80–100', the upward motion of the heavy particle would be similar in character to that of an ejected fluid lump, provided that the parameter $w/\kappa u_*$ does not exceed the value after which observations show no suspension of particles. This implies that the upward motion of a particle originating in the region $0 < y^+ < 50$ is strongly controlled by the bursting flow until the burst breaks up and that the upward motion of the particle then terminates at a y^+ of 100–200. From this position the particle returns to the region near the bottom. In this downward motion of the particle, the fluid instantaneously in the particle's immediate neighbourhood appears to be high-speed fluid penetrating towards the wall (the sweep zone), since the conditionally averaged streamwise velocity profile (figure 7) corresponding to the particle fall shows an excess relative to the mean velocity profile. It should be noted that a similar trend was observed also by Grass (1976, private communication). In Offen & Kline's model, a particle on the way back to the wall is expected to meet the next lifting wall streak (i.e. the ejected fluid due to the next burst). This may cause the particle to have another upward motion. Or else, if the particle reaches the bottom, it will eventually be lifted up from the bottom and have another upward motion similar to the one explained in the preceding paragraphs. It is this process close to the bottom in turbulent flows which would make it possible for heavy particles to stay in suspension.

Observations show that particles, especially relatively lighter ones, can stay in suspension at heights much greater than $y^+ \sim 200$. This implies that for particle suspension in the region further out there must be some other mechanism. The transverse vortices and large-scale flows in the outer region, which are two subsequent events in the deterministic sequence of events in turbulent boundary layers and have recently been observed by Nychas *et al.* (1973), could be the agents responsible for particle suspension in this region. Grass' (1974) relevant proposals also favour this scheme.

4.3. *Discussion*

Sutherland (1967) proposed a mechanism for the particle entrainment, which has already been mentioned in § 1. Sutherland considered particle lift-up to be due to what he called an incoming eddy from further upstream. This eddy rotates in such a way that the flow along its lowermost portion is in the direction of the mean flow. He suggested that, when such an eddy disrupting the viscous sublayer impinges on the particle, it will exert a drag force on the particle in the direction of the local velocity, which, as a result of the rotation within the eddy, is inclined at a small angle to the bed. Sutherland then suggested that an exposed particle can be expected to be lifted up from the bed when the vertical component of the drag force associated with the eddy exceeds the particle's immersed weight plus any forces arising from interference with neighbouring grains. Going one step further, Sutherland assumed a particle suspension as follows. A particle lifted up from the bottom is projected along a path inclined at a small angle to the bed. Pointing out that at a distance from the bed approximating the sublayer thickness the grain can be influenced by the turbulent fluctuation of the main flow, Sutherland suggested that 'suspension is then a question of whether or not an upward velocity in excess of the grain's fall velocity occurs before the grain settles back to the bed'.

The present mechanism differs from Sutherland's mechanism mainly in the following three points.

(*a*) In both, there exists a rotating structure. But the one in the present mechanism, the so-called recirculation cell, rotates in the opposite direction to that in Sutherland's. Note that the former, being part of the Offen & Kline's model, is consistent with the trends in all the relevant data.

(*b*) In the case of a single particle on the smooth bottom of an open channel, Sutherland's mechanism implies that the lift-up of the particle occurs when the vertical component of the drag force due to an incoming eddy in contact with the particle exceeds the particle's immersed weight. The present mechanism views the particle lift-up as a result of the local temporary adverse pressure gradient imposed on the particle by the recirculation cell passing overhead, which is the counterpart of the Sutherland's incoming eddy.

(*c*) Sutherland's mechanism views the particle suspension in the conventional way, i.e. suspension is a matter of having an upward turbulent velocity in excess of the particle's fall velocity, whereas the present paper suggests that the particle is maintained in suspension close to the bottom owing to the bursting flow structure.

The observations and the proposed mechanism of the present work appear to be in qualitative agreement with Engelund's analysis (1970), which has been introduced briefly in § 1. Indeed, the present observations showed that most of the downward motion of particles terminated before the particles reached the bottom, which, in the proposed model, is thought to be because the particles meet the next lifting wall streak. This is in agreement with Engelund's prediction that the central part of the wall region constitutes a barrier against settling.

The present study agrees with many aspects of Grass' (1974) experiments and his proposals concerning sediment suspension mechanics. Grass used fine sand as a tracer in a flat-plate turbulent boundary layer with a hydraulically smooth boundary. The motion film used by Grass to record details of the suspension process revealed most

of the details of the flow structure (visualized by the sand) shown up by earlier visualization observations (e.g. Grass 1971; Nychas *et al.* 1973; Offen & Kline 1973; and others). Grass' work thus directly established the link between the two processes of fluid ejection and particle suspension. Finally, Jackson (1976, p. 554) noted that 'a plausible candidate for the suspension mechanism is the bursting process', presenting a review of scattered observations on sediment dispersal from the bed which provided qualitative support for his suggestion.

5. Conclusions

As has been mentioned above, observations made in a laboratory channel show that a small heavy particle may be lifted up from the bottom by the flow and can be maintained in suspension, despite the strong tendency for the particle to be lost from the flow by gravitational fall-out. In this study, (*a*) observations of the motion of such particles were made and (*b*) an attempt was made to explain the mechanism of particle suspension.

The present observations showed that a particle which started to travel upwards from the region $0 < y^+ < 50$, which is part of the wall region where fluid ejections originate, could reach a y^+ of 100–200 in a single continuous motion. The particle was observed to return towards the wall after its upward motion terminated. The downward motion of the particle continued down to a relatively small y^+ in the wall region, sometimes terminating at the wall, from which the particle started another upward motion. The data obtained from the observations were used to predict the probability density function of the vertical position of particles and also to predict the average velocity of individual particles in both their upward and their downward trajectories. The results seem to be consistent with the information at present available.

Making use of the present observations of the particle motion and following Offen & Kline's (1975) model of the bursting process, an attempt was made to explain the particle suspension mechanism close to the bottom in turbulent flows. The proposed mechanism views the particle lift-up from the bottom as a result of the temporary local adverse pressure gradient which is imposed on the particle by the burst passing overhead. According to the mechanism, the rise of the lifted particle is strongly controlled by the bursting flow structure, which enters the main body of the flow together with the particle owing to the same adverse pressure gradient. This control continues until the accompanying bursting flow structure breaks up; the particle rise then terminates and the particle starts to return to the neighbourhood of the wall. On the way back to the wall, it is expected to meet fresh lifting fluid due to the next burst from further upstream, or else, in the case where the particle reaches the bottom, it is lifted up into the body of the flow by the same mechanism as was explained above. This will cause the particle to have another upward motion. This process makes it possible for the particle to stay in suspension.

We wish to express our thanks to Dr A. J. Grass of University College London for his comments on the first draft of the paper.

REFERENCES

BATCHELOR, G. K. 1965 *Proc. 2nd Austr. Conf. Hydraul. Fluid Mech.* p. 19.

BATCHELOR, G. K., BINNIE, A. M. & PHILLIPS, O. M. 1955 *Proc. Phys. Soc.* B **68**, 1095.

BRODKEY, R. S., WALLACE, J. M. & ECKELMANN, H. 1974 *J. Fluid Mech.* **63**, 209.

CORINO, E. R. & BRODKEY, R. S. 1969 *J. Fluid Mech.* **37**, 1.

ELDER, J. W. 1959 *J. Fluid Mech.* **5**, 544.

ENGELUND, F. 1970 *Basic Res. Prog. Rep. Hydraul. Lab., Tech. Univ. Denmark* **21**, 7.

ENGELUND, F. & GRAVESEN, H. 1972 *Basic Res. Prog. Rep. Hydraul. Lab., Tech. Univ. Denmark* **27**, 33.

GRASS, A. J. 1971 *J. Fluid Mech.* **50**, 233.

GRASS, A. J. 1974 *Euromech* 48, *Inst. Hydrodyn. Hydraul. Engng Tech., Univ. Denmark*, p. 33.

HENDERSON, F. M. 1966 *Open Channel Flow*. Macmillan.

JACKSON, R. G. 1976 *J. Fluid Mech.* **77**, 531.

MONIN, A. S. & YAGLOM, A. M. 1971 *Statistical Fluid Mechanics: Mechanics of Turbulence*, vol. 1. MIT Press.

NYCHAS, S. G., HERSHEY, H. C. & BRODKEY, R. S. 1973 *J. Fluid Mech.* **61**, 513.

OFFEN, G. R. & KLINE, S. J. 1973 Experiments on the velocity characteristics of 'bursts' and on the interactions between the inner and outer regions of a turbulent boundary layer. *Dept. Mech. Engng, Stanford Univ. Rep.* MD-31.

OFFEN, G. R. & KLINE, S. J. 1974 *J. Fluid Mech.* **62**, 223.

OFFEN, G. R. & KLINE, S. J. 1975 *J. Fluid Mech.* **70**, 209.

SUMER, B. M. 1974 *J. Fluid Mech.* **65**, 11.

SUMER, B. M. 1977 *Hydraulic Problems Solved by Stochastic Methods. Proc. 2nd Int. IAHR Symp. Stochastic Hydraul., Lund (Sweden)* (ed. P. Hjorth, L. Jönsson & P. Larsen), paper 9. Water Resources Publ., Fort Collins, Colorado.

SUTHERLAND, A. J. 1967 *J. Geophys. Res.* **72**, 6183.

WILLIAMS, P. B. & KEMP, P. H. 1971 *Proc. A.S.C.E., J. Hydraul. Div.* **97**, 505.

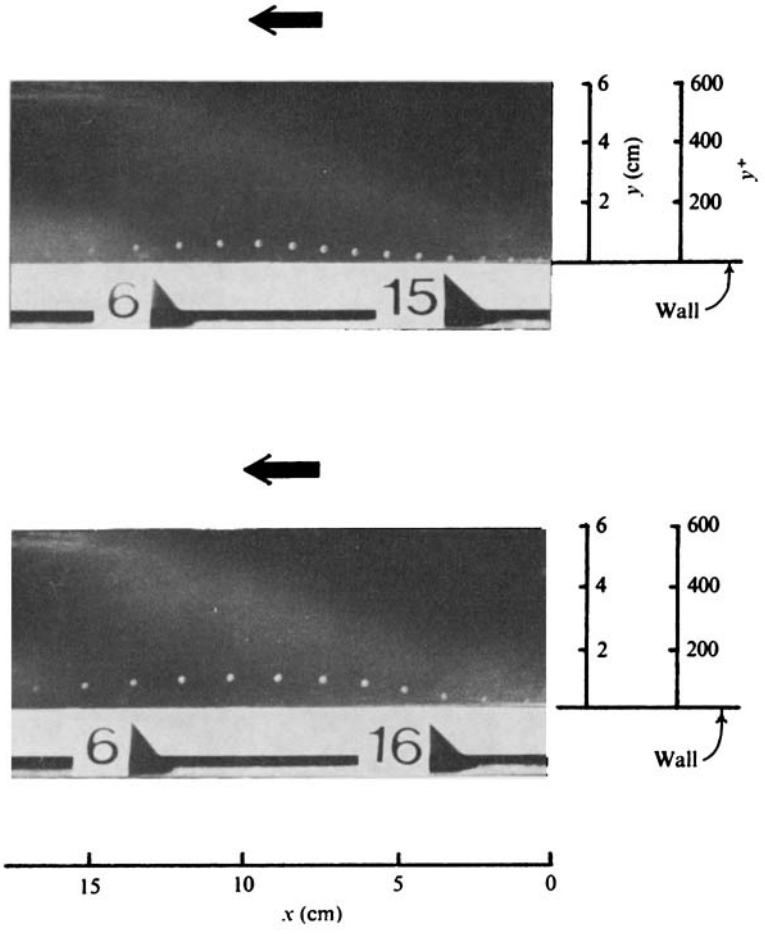

FIGURE 4. Typical particle paths recorded by the fixed camera system. Particle *C*. Exposures are spaced 0·086 s apart. Note that the particle images are accurately recorded in both the x and the y direction.